A novel synthetic approach to tune the surface properties of polymeric films: Ionic Exchange Reaction between Sulfonated Polyarylethersulfones and Ionic Liquids

V. Sabatini[1,2], H. Farina[1,2], A. Montarsolo[3], S. Ardizzone[1,2], M. A. Ortenzi[1,2]

[1]Department of Chemistry, University of Milan, Milan, Italy, [2]CRC Materiali Polimerici (LaMPo), Dipartimento di Chimica, Università degli Studi di Milano, Milano, Italy, [3]CNR ISMAC (National Research Council – Institute for Macromolecular Studies), Biella, Italy

Corresponding Author to Marco Aldo Ortenzi. E-mail: marco.ortenzi@unimi.it

Abstract

Currently, no studies dealing with the role played by Ionic Liquids (I.Ls.) on tailoring surface features of polymer films are available. In this work, I.Ls. influence on the surface of Sulfonated Polyarylethersulfones (SPESs) was investigated. SPESs with different degrees of sulfonation (DS) were synthesized; their surface properties were modulated through an ionic exchange reaction between the K^+ cation of SPESs and I.Ls. synthesized changing the length of cation apolar groups.

Hydrophobic properties of SPES_I.Ls. films improve with both the increase of DS and the length of I.Ls. alkyl chains due to higher surface roughness, as shown by SEM and AFM.

GRAPHICAL ABSTRACT

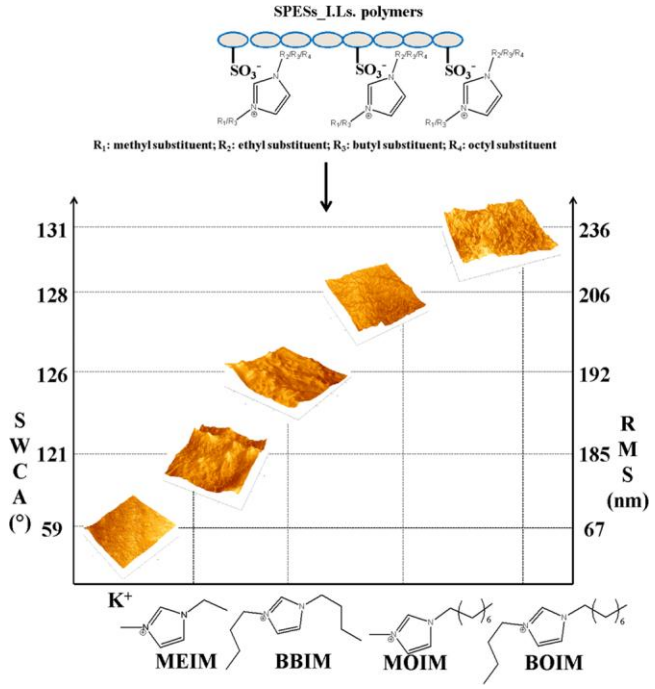

KEYWORDS: sulfonated polyarylethersulfone; ionic liquid; cation exchange reaction; surface roughness; hydrophobic film.

1. INTRODUCTION

Surface properties, such as wettability, morphology and surface chemistry, play a crucial role in designing possible application fields of a polymeric material. Surface wettability is among the most important characteristics useful to determine potential application of a polymeric material. In fact, material wettability and the modulation of wetting properties play a key role in the development of new polymeric materials for a very large number of industrial applications, i.e. the fields related to coating [1], printing [2], filtration membranes [3] and biomedical devices [4].

Surface chemical modification and/or mechanic-physical interfacial one of polymeric materials are effective in tailoring the properties of the material in a number of different ways providing, for instance biocompatibility or anti-microbial properties, for uses in sensor applications [5] or as support for metal layers deposition [6]. Furthermore, by tuning the surface roughness of polymeric surfaces, adhesion can be controlled with respect to different environments and materials [7].

The wetting properties of solid surfaces are affected by both their intrinsic chemical composition and by their morphology [8]; for example hydrophobic surfaces roughened on purpose can become super hydrophobic, showing an efficient mechanism of self-cleaning [9].

The chemical composition of a surface defines its hydrophobic or hydrophilic behavior. In addition, the final observed hydrophilic or hydrophobic property depends on the surface topography. Promoting a specific roughness allows a substantial enhancement of these intrinsic properties to be obtained. As widely described in literature, starting from Wenzel description of the wettability, an increase in roughness for an hydrophobic surface provokes an increase in the contact angle and consequently in the hydrophobic properties, on the grounds of the following equation: $\cos \theta_w = r \cos \theta_y$ where θ_w is the Wenzel contact angle, r is the roughness factor and θ_y the contact angle of the ideal smooth surface (Young contact angle) [10,11].

Up to now, many methods have been developed to produce rough polymeric surfaces with different types of polymers including solidification of melted alkyl ketene dimers [12], plasma polymerization/etching of polypropylene (PP) in the presence of polytetrafluoroethylene (PTFE) [13], microwave plasma-enhanced chemical vapor deposition [14], anodic oxidization of aluminium [15], immersion of porous alumina gel films in boiling water [16], phase separation [17] and molding [18]. These methods are often complex and can be applied only to specific polymers, such as polyethers, polyesters and polycarbonates. Furthermore, to obtain self-cleaning surfaces, coating with low surface energy materials, such as fluoroalkylsilane, is often necessary [19].

Sulfonated Polyarylethersulfone (SPES) has received great attention in the last decade due to the possibility to use it for a variety of separation processes, e.g. ion exchange membranes [20], reverse osmosis [21] and electro dialysis process [22]. It is a completely amorphous polymer, characterized by excellent UV and thermal resistance (e.g. high glass transition temperature, T_g, up to 230°C and low thermal expansion coefficient), optical properties (refractive index: n=1.63 at λ=589.3 nm), chemical stability [23], oxidation resistance [24], as well as by good mechanical properties [25] and easy processability [26]. SPESs can be prepared via two different synthetic routes; one is the synthesis of Polyarylethersulfone (PES) followed by post-sulfonation reaction with sulfonating agents, commonly defined as "heterogeneous synthesis" [27], the other uses pre-sulfonated monomers in the feed of the polymerization reaction and is defined "homogeneous synthesis" [28]. Homogeneous synthesis is preferable because it allows a

good control of the macromolecular architecture [29] and of the sulfonation degree (DS) of the polymer [30].

In a previous work by our group, we have studied the wettability of SPES films having different DS, obtained by solvent casting deposition onto a PTFE support. Wetting properties of both sides of these films, the air-side and the PTFE one, are characterized by decreasing static water contact angles (SWCA) as the DS increase; the PTFE-mold side shows slightly higher SWCA [31].

In order to investigate new solutions for the development of hydrophobic materials, Ionic Liquids (I.Ls.) are interesting candidates for this purpose. I.Ls. are a class of molten salts usually composed by linear or cyclic ammonium cations, imidazolinium and pyridinium being the ones most commonly reported in literature, thanks to their easy preparation [32]. It is known that I.Ls. have excellent thermal stability (up to 400°C) [33] and that their physical-chemical properties can be modulated by changing the nature of the cation or anion [34]. In fact, the modulation of non-polar groups on the cation, characterized by strong hydrophobic properties, can produce major changes in the tendency of I.Ls. to modify the efficiency of ion packing and therefore in their hydrophobic features; increasing the length of alkyl chains, the hydrophobic properties of the salt increase [35].

With the aim to prepare a double side self-cleaning polymeric material, we performed an ionic exchange reaction between the potassium cation of SPES sulfonic moieties and two I.Ls. characterized by apolar alkyl chains with different length, 1-Ethyl,3-Methyl

Imidazolinium methyl sulfite (MEIM) and 1,3-Dibutyl Imidazolinium bromide (BBIM). In this case, both side of the polymeric films showed higher SWCA than SPES alone, especially on the PTFE-side [36].

In order to investigate the above reported effects and to assess whether the functionalization by I.Ls. did introduce modulation of the morphological features of the polymeric materials, other two new I.Ls. with increasing length of the cation alkyl chains were prepared, 1-Methyl,3-Octyl Imidazolinium bromide (MOIM) and 1-Butyl,3-Octyl Imidazolinium bromide (BOIM). After cation-exchange reaction of I.L.s with SPES having DS ranging from 0.5 to 1.0 meq $SO_3^-*g^{-1}$ of polymer, their quantity in SPESs was determined by ^1H NMR spectroscopy and the thermal properties of the resultant polymeric materials were evaluated by DSC.

The effect of the four I.Ls. on wetting, morphology and surface roughness of SPES_I.Ls. membranes, obtained via solvent casting deposition, were studied by SWCA analyses, Scanning Electron Microscopy (SEM), Atomic Force Microscopy (AFM) and Fourier Transform (FT) Infrared (IR) spectroscopy.

The polymeric films based on SPES and I.Ls. prepared in this work could be, in a future, used as innovative self-cleaning materials for a very large number applications, including covers for solar cells.

2. EXPERIMENTAL

2.1. Materials

4,4'-difluorodiphenylsulfone (BFPS, ≥99%) and 4,4'–dihydroxydiphenyl (BHP, ≥97%) were supplied by Sigma Aldrich; 2,5-dihydroxybenzene-1-sulfonate potassium salt (sulfonated hydroquinone, SHQ, ≥98%) was obtained from Alfa Aesar and potassium carbonate (K_2CO_3, ≥98% anhydrous) was purchased from Fluka; all the reagents were dried at 30°C in vacuum oven (about 4 mbar) for at least 24 hr before use and employed without further purification. 1-methylimidazole (≥99%), 1-butylimidazole (≥98%), butyl bromide (≥99%) and octyl bromide (≥99%) were obtained from Sigma Aldrich and used as received. N-methyl-2-pyrrolidone (NMP, ≥99.5% anhydrous), dimethylacetamide (DMAc, ≥99.5%), N, N-dimethylformamide (DMF, 99.8% anhydrous), toluene (99.8% anhydrous), acetonitrile (99.8% anhydrous), ethyl acetate (99.8% anhydrous), distilled water Chromasolv® (≥99.9%), dimethyl sulfoxide-d_6 (DMSO-d_6, 99.96 atom % D) and deuterium oxide (D_2O, 99.9 atom % D) were supplied by Sigma Aldrich and used without purification.

2.2. Synthesis Of Sulfonated Polyethersulfones (Spess)

Three SPESs with increasing nominal DS, expressed as meq $SO_3^-*g^{-1}$ of polymer, -SPES_0.5, SPES_0.75, SPES_1- were synthesized. The exact amount of the monomers used for the syntheses are reported in Table 1. In a representative polymerization procedure, BFPS, BHP, SQH and K_2CO_3, the latter used as proton scavenger, are introduced into a 100 cm^3 one neck round-bottom flask equipped with magnetic stirring. Toluene and NMP are loaded in order to have a 10% mass/volume concentration of the reactants in the solution. The flask, equipped with a modified Dean-Stark device and

under nitrogen atmosphere, is put in an oil bath and the mixture is maintained under reflux for 6 hr; the residual hydration water is removed as an azeotrope with toluene through the modified Dean-Stark device. After complete water removal, the temperature is gradually increased to 198°C and then the reaction mixture is kept 18 hr at 198°C.

The hot viscous dark-purple solution obtained is precipitated into a large excess of water under stirring and a light-yellow solid precipitated is obtained. The solid is recovered via filtration and then residual monomers and K_2CO_3 are removed carefully washing the solid with water; this purification procedure is repeated for several times. The resultant polymer is dried in a vacuum oven (about 4 mbar) at 50°C for 24 hr. Real DS is quantitatively measured via ^{1}H NMR, calculating the integral ratios (see Figure 2) between the proton in ortho to the sulfonic group **[g]** of SHQ and the ones of BFPS **[d], [f]** and of BHP **[a]**, using *Equation 1*:

$$DS = \frac{Ig*1000}{\left(\frac{Id,f*UrBFPS}{4}\right)+\left(\frac{Ia*UrBP}{4}\right)+ Ig*UrSHQ} \qquad (1)$$

where *Ig* is the integral area of peak **[g]**; *Id,f* is the total integral area of the peaks **[d]** and **[f]**; *Ia* is the integral area of the peak **[a]**; *UrBFPS* corresponds to the molecular weight of BFPS repeat unit (216.25 g*mol^{-1}); *UrBP* corresponds to the molecular weight of BP repeat unit (184.21 g*mol^{-1}) and *UrSHQ* corresponds to the molecular weight of SHQ repeat unit (226.26 g*mol^{-1}).

2.3 Synthesis Of Ionic Liquids (I.Ls.)

Four Imidazolinium based I.Ls. were synthesized: 1-Ethyl,3-Methyl Imidazolinium methyl sulfite(MEIM), 1,3-Dibutyl Imidazolinium bromide (BBIM), 1-Methyl,3-Octyl Imidazolinium bromide (MOIM) and 1-Butyl, 3-Octyl Imidazolinium bromide (BOIM); the syntheses were performed according to previously reported procedures [37].

For the syntheses of MEIM and BBIM, respectively methyl ethyl sulphite (2.03 g) and 1-methylimidazole (1.25 g) for MEIM and 1-bromobutane (2.55 g) and 1-butylimidazole (1.89 g) for BBIM, are introduced in a 100 cm^3 one-neck round bottom flask equipped with magnetic stirring; the flask, under nitrogen atmosphere, is put in an oil bath and the synthesis is kept for 1 hr at 110°C and then cooled to room temperature. The product is purified from the unreacted monomers thanks to several washings with water.

The syntheses of MOIM and BOIM were conducted as follows: a 100 cm^3 three-necked round bottom flask is equipped with a nitrogen inlet adapter, an internal thermometer adapter, an overhead mechanical stirrer and a reflux condenser. The flask is flushed with nitrogen, charged with 20 cm^3 of acetonitrile and respectively with octyl bromide (3.59 g) and 1-methylimidazole (1.25 g) for MOIM and with octyl bromide (3.59 g) and 1-butylimidazole (1.89 g) for BOIM, and brought to reflux in an oil bath. The solution is heated under reflux for 48 hr and then cooled to room temperature. Volatiles are removed from the resulting yellow solution under reduced pressure (about 4 mbar). The remaining light-yellow oil is re-dissolved in acetonitrile (20 cm^3) and added drop wise via cannula in a 250 cm^3 one-necked round bottom flask of a well-stirred solution of 100 cm^3 of ethyl

acetate. The imidazolinium salt begins to crystallize almost immediately and, after the addition of the acetonitrile solution is completed, the flask is cooled at -30°C for 12 hr. The supernatant solution is removed via filtration through a filter cannula and the resulting white solid is dried under pressure (about 4 mbar) at 30°C for 6 hr. The structure of the products obtained is determined via ^{1}H NMR: Figure 1 shows the structures and abbreviations of all the ions used in this work.

2.4 Synthesis Of Spess With I.Ls.

An ionic exchange reaction between the K^{+} cation of SPESs and the cations of the four I.Ls. synthesized was conducted. The exact amount of the reagents used for the syntheses is reported in Table 2. In a representative synthesis procedure, the cation exchange reaction was performed as follows: SPES and I.L. are introduced in a one-neck round bottom flask containing DMAc (15 cm^{3}) equipped with magnetic stirring; the flask is transferred to the oil bath and the synthesis is kept under nitrogen atmosphere for 24 hr at 110°C.The reaction mixture is then precipitated into a large excess of water and recovered via filtration; the product is purified from the residual reagents thanks to several washings with water. The resultant polymer is finally collected by filtration and fully dried in a vacuum oven (about 4 mbar) at 50°C for 24 hr. The rate of substitution (RS) is measured via ^{1}H NMR.

2.5 Characterization Of Polymers

2.5.1 Nuclear Magnetic Resonance: ^{1}H NMR

^{1}H NMR spectra were collected at 25°C with a BRUKER 400 MHz spectrometer. Samples for the analyses were prepared dissolving 10-15 mg of SPESs or SPES_I.Ls. samples in 1 cm^3 of DMSO-d_6 and 8-10 mg of I.Ls. in 1 cm^3 of D_2O.

2.5.2. Intrinsic Viscosity (IV)

The intrinsic viscosity of SPESs samples was measured using an Ubbelohde viscometer in a thermostatic water bath at 25°C. Polymers were dissolved in dimethylacetamide and analysed in the concentration range 1-0.3 $g*dL^{-1}$.

2.5.3. Size Exclusion Chromatography (Sec)

The molecular weight of SPESs samples was evaluated using a SEC system consisting of a Waters 1515 Isocratic HPLC pump, three Waters Styragel columns set (HR3-HR4-HR5), and a Refractive Index (RI) detector Waters 2487 Detector. Analyses were performed at room temperature, using a flow rate of 1 cm^3/min and 40 μL as injection volume. Samples were prepared by dissolving 40 mg of polymer in 1 cm^3 of anhydrous DMF; before the analysis, the solution was filtered with 0.45 μm filters. Molecular weight data were expressed in polystyrene (PS) equivalents. The calibration was built using monodispersed PS standards having the following nominal peak molecular weight (Mp) and molecular weight distribution (D): Mp = 1600000 Da (D≤1.13), Mp = 1150000 Da (D≤1.09), Mp = 900000 Da (D≤1.06), Mp = 400000 Da (D≤1.06), Mp = 200000 Da (D≤1.05), Mp =90000 Da (D≤1.04), Mp =50400 Da (D=1.03), Mp= 30000 Da (D=1.06), Mp = 17800 Da (D=1.03), Mp = 9730 Da (D=1.03), Mp = 5460 Da (D=1.03), Mp = 2032 Da (D=1.06), Mp = 1241 Da (D=1.07), Mp = 906 Da (D=1.12), Mp = 478 Da (D=1.22);

Ethyl benzene (molecular weight = 106 g/mol). For all analyses, 1,2-dichlorobenzene was used as internal reference.

2.5.4. Differential Scanning Calorimetry (Dsc)

DSC analyses were conducted using a Mettler Toledo DSC 1, on samples of SPESs and SPES_I.Ls. weighting from 5 to 10 mg each. Temperature program was divided in five parts:

i) heating from 25°C to 330°C at 10°C/min;

ii) 5 min of isotherm at 330°C;

iii) cooling from 330°C to 25°C at 10°C/min;

iv) 5 min isotherm at 25°C;

v) heating from 25°C to 330°C at 10°C/min (T_g was measured here).

2.6 Preparation Of Spess And SPES_I.L. Membranes

Given the difficulties in completely removing solvents like NMP, toluene and DMAc from SPESs and SPES_I.Ls., the polymers were repeatedly washed with water for several days under stirring, dried in a vacuum oven (about 4 mbar) at 50°C for 24 hr and then the absence of residual solvent was checked via isothermal TGA (2 hr at 250°C under nitrogen flow). Polymers weights obtained after TGA analyses are reported in Supporting Information. Membranes of both SPESs and SPES_I.Ls. were obtained via solution casting: polymers were dissolved in DMAc using 21% mass/volume concentration and the corresponding solutions were cast onto a PTFE substrate. The solvent was evaporated

for 24 hr in vacuum oven (about 4 mbar) at 40°C; the absence of residual solvent was checked via isothermal TGA (2 hr at 250°C under nitrogen flow) and membranes weights obtained after TGA analyses are reported in Supporting Information. In all cases, residual weight is very close to 100% and can be considered within the experimental error, confirming that solvents were removed both from the polymers and from membranes.

Membranes thickness was in the range 120-125 μm; it was evaluated by Nikon eclipse ME600 optical microscope with Nikon digital camera light DS_Fi1, software Nis-Elementi BR, magnification 50X.

2.7 Characterization Of The Membranes

2.7.1 Static Water Contact Angle (Swca)

Surface wetting properties of the membranes surface were assessed by contact angle measurement using a Krüss Easydrop Instrument, attaching a 4*4 cm membrane on a glass slide. For the measure, a total of 1 μL of double distilled water was dropped on the air-side surface of the membranes. At least five measurements were taken on each sample to get reliable values. The measurements error was ±3°. The same procedure was performed on the PTFE-side surface of the membranes.

2.7.2 Scanning Electron Microscopy (Sem)

SEM studies were carried out by a Leica Electron Optics 435 VP microscope. The investigations were performed with an acceleration voltage of 15 kV, 50 pA of current probe, and 20 mm of working distance. The samples were mounted on aluminium

specimen stubs with double-sided adhesive tape and sputter-coated with a 20 nm thick gold layer in rarefied argon, using an Emitech K550 Sputter Coater, with a current of 20 mA for 180 s.

2.7.3 Atomic Force Microscopy (Afm)

AFM characterizations were carried out with a Nano-R2 AFM produced by Pacific Nanotechnology (USA) and were evaluated from 10 μm^2 images. The AFM imaging technique used was Close Contact mode and APPNANO (USA) highly doped single crystal silicon probes of 125 μm nominal length were used. Data were acquired by means of SPM Cockpit Software, processed and analysed by Nanorule+ software, both equipped with the Nano-R_2 system. Surface roughness was measured by image analysis of 10 μm*10 μm areas and expressed as root-mean-square (RMS).

2.7.4 Fourier Transform-Infrared (Ft-Ir)

The presence of different hydrophobic I.Ls. on the surface of both sides (mold-side and air-side) of the polymeric membranes prepared was checked by FT-IR spectroscopy, performed on a Spectrum 100 spectrophotometer (Perkin Elmer) in attenuated total reflection (ATR) mode using a resolution of 4.0 and 256 scans, in a range of wavenumber between 4000 and 400 cm^{-1}. A single-bounce diamond crystal was used with an incident angle of 45°.

3. RESULTS AND DISCUSSION

3.1 Synthesis And Characterization Of Spess

SPESs with three nominal DS -0.5-0.75-1.0- were synthesized; Scheme 1 shows the representative procedure for the homogeneous synthesis of SPESs by direct co-polymerization of BFPS and BHP with a sulfonated monomer, SHQ; the full description of SPESs homogeneous synthesis and their macromolecular characterizations are reported in previous works [31, 36].

Figure 2 reports ^{1}H NMR spectrum of SPES with a nominal DS of 0.5 meq $SO_3^-*g^{-1}$ of polymer.^{1}H NMR spectra of SPES_0.75 and SPES_1 are reported in Supporting Information.

A list of SPESs synthesized and the DS obtained as reported in 2.2 paragraph, are shown in Table 3; results indicate that the sulfonated monomer successfully reacted in all the SPESs synthesized.

Since molecular weight strongly affects the possibility to form membranes, the molecular weights of SPESs samples were measured via intrinsic viscosity (IV) and Size Exclusion Chromatography (SEC) analyses. IV is commonly used to characterize SPES: when dealing with ionic polymers such as SPES, it is well known that polyelectrolyte effect appears when macromolecules are diluted in solution. This effect leads to higher values of reduced viscosity as the concentration of the polymer in the solvent gets lower, due to charge repulsion. Therefore dilute solution viscosities of polyelectrolytes should be measured in the presence of a low-molar mass salt, which is able to neutralize charges [38].

In a previous work of our group [31], IV of SPESs polymers was measured in DMAc both with and without LiBr in the concentration range from 1.0 g*cm^3 to 0.3 g*cm^3. Data showed no significant differences between the values obtained with and without LiBr, suggesting that the polyelectrolyte effect might depend on the amount of $SO_3^-K^+$ groups present in the polymer chains and that this effect is absent SPESs with low amounts of sulfonic groups, i.e. with low DS. SPESs IV resulted to span from 0.34 to 0.72 dL*g^{-1}.

Number average molecular weights ($\overline{Mn}$), weight average molecular weights ($\overline{Mw}$) and molecular weight distribution (D) of SPES samples were determined via SEC and expressed as polystyrene equivalents. IV data and SEC values, shown in Table 3, obtained are consistent with the results reported by other authors in previous works [39,40], confirming that SPESs samples characterized by high molecular weights were synthesized.

To assess the thermal properties of SPES samples, DSC analyses were performed. As reported in several works [41], SPESs are characterized by very high T_g and consequently they can be widely used in advanced separation technologies, including as a low-cost alternative to expensive fluorinated polymers in fuel cells, biomedical field (such as artificial organs) and medical devices used for blood purification, fields in which high thermal resistances are requested [42].

As reported in Table 3, SPESs synthesized have excellent T_g values that increase as the DS increases: SPES_0.5 T_g is 259.7°C, a value that increases up to 290.9°C for

SPES_0.75 and to 303.6°C for SPES_1. DSC thermograms of SPES_0.5, 0.75 and 1 are reported in Supporting Information.

As general statement, T_g tends to increase with the increased amount of SO_3^- groups introduced into the polymer chains. The phenomenon is due to the increasing quantity of SHQ present in the polymer, since this molecule is characterized by a rigid and bulky structure [43].

3.2 Cation Exchange Reaction And Characterization Of SPES_I.Ls.

In order to produce meaningful comparisons among films obtained from SPES_I.Ls., all the I.Ls. samples were freshly prepared on purpose. ^{1}H NMR spectra obtained of MEIM, BBIM, MOIM and BOIM are shown in Supporting Information.

Ionic exchange reactions between the potassium cation of SPESs and the imidazolinium cations of MEIM, BBIM, MOIM and BOIM were conducted. Scheme 2 shows the representative procedure for the cation exchange reaction of SPESs with I.Ls.; in Figure 3 a ^{1}H NMR spectrum collected on the material after the ionic exchange reaction between SPES_0.5 and MEIM is reported. Other SPES_I.Ls. ^{1}H NMR spectra are shown in Supporting Information. A list of the samples synthesized with the rate of substitution (RS) obtained and T_g is shown in Table 4.

To assess the possible application temperature range of SPES_I.Ls., DSC analyses were performed. As shown in Table 4, SPESs with I.Ls. have a T_g similar to the ones of SPESs

samples reported previously in Table 3, suggesting that the ionic exchange reaction does not significantly affects the excellent thermal properties of these materials.

3.3 Membranes Characterization: SWCA, SEM And AFM Analyses

3.3.1 Static Water Contact Angle Analyses (SWCA)

Static water contact angles of membranes of SPESs and SPES_I.Ls., obtained from solution casting in DMAc, were evaluated. The samples were cast onto a PTFE substrate: wetting properties were measured both at the air-side surface and at the PTFE-side surface of the membranes. Table 5 shows the results obtained.

Contact angles of SPESs decrease as the quantity of $-SO_3^-K^+$ groups increases, due to the high polarity of the $–SO_3^-$ groups. The increase of θ_w observed on the PTFE-side for SPES membranes with respect to the air-side is probably due to the organization of the $SO_3^-K^+$ groups of the polymeric chains occurring during the evaporation of the solvent and to the interaction with the high hydrophobic PTFE mold surface. Therefore, as reported for θ_w observed on the air-side of SPES membranes, the water contact angles significantly decrease with the increase of SPES DS.

After cation exchange reaction between SPESs and I.Ls., the values of static water contact angles dramatically change: thanks to the addition of I.Ls., the hydrophobic properties measured on the PTFE-side surface increase as the quantity of sulfonated groups increases, due to the higher number of I.L. exchanged. Increasing the length of the apolar alkyl chains of the imidazolinium cations, the static water contact angles increase:

θ_w of SPES_MEIM_0.5 is $\overline{108}°$, a value that increases up to $\overline{123}°$ for SPES_BBIM_0.5, to $\overline{124}°$ for SPES_MOIM_0.5 and up to $\overline{130}°$ for SPES_BOIM_0.5.

The measurements of the static water contact angles on the air-side have not revealed significant differences between different DS and length of the imidazolinium alkyl chains.

In order to explain the difference between air-side and PTFE-mold side SWCA data, a hypothesis that can be done is that, during the evaporation of the solvent, the apolar SO_3^- I.Ls$^+$. groups in contact with a hydrophobic surface -the PTFE mold - are orientated towards the hydrophobic surface, since they are less affine to the solvent. Thanks to the selective orientation of the imidazolinium alkyl chains on the PTFE-side surface of SPES_I.L. membranes, the mold-side is characterized by higher SWCAs, ranging from $\overline{108}°$ to $\overline{131}°$, than the ones measured at the air-side of the membranes themselves.

3.3.2 Scanning Electron Microscopy Analyses (SEM)

SEM analyses for SPESs and SPES_I.Ls. samples were performed in order to clarify the influence of different hydrophobic I.Ls. on the surface properties of the polymeric membranes prepared. Figure 4 presents the morphologies of representative membranes from both air-side and PTFE-side of SPESs and SPES_I.Ls. samples.

In the case of SPES_1, no surface differences are detectable between the air-side (*4a*) and the mold-side of the polymeric membrane (*4b*). When I.Ls. are added, it is possible to

observe that the surface at the air-side remains smooth (*4c*), while the surface at the mold-side of the membrane changes from smooth to rough (*4d*).

The roughness of the PTFE-side of SPES_I.Ls. membranes increases as the DS of SPESs increases, i.e. with the number of hydrophobic I.Ls. cations exchanged, as it is possible to observe comparing SPES_MEIM_0.5 (*4d*) with SPES_MEIM_0.75 (*4e*) and SPES_MEIM_1 (*4f*), and it enhances as the length of the imidazolinium alkyl chains enhances, as shown in Figure 4f for SPES_MEIM_1, in Figure 4g for SPES_BBIM_1, in Figure 4h for SPES_MOIM_1 and in Figure 4i for SPES_BOIM_1. SEM analyses of SPES_I.Ls. air-side samples are reported in Supporting Information. SEM images are in good agreement with SWCA data reported in paragraph 3.3.1. These results are due to the selective orientation of the imidazolinium alkyl chains on the hydrophobic PTFE mold during the evaporation of the solvent, thus changing the membranes surface in correspondence of the PTFE-side from smooth to rough and promoting the formation of highly hydrophobic surfaces.

3.3.3 Atomic Force Microscopy Analyses (AFM)

It is well known that wetting of a surface by a solvent is affected by the roughness of the surface itself [39]; the effect of roughness on the wetting properties of some representative membranes of both unmodified SPESs and SPES_I.Ls. samples, presented in Figure 5, has been examined by AFM analyses; the corresponding RMS roughness values, measured using the software described in 2.7.3 paragraph, are reported in Table 6.

Comparing AFM topographies of the mold-side of pristine SPES (Figure 5a) and SPES_I.Ls. samples (Figure 5b, c, d, f, g and h), it is clear that the surfaces of SPES_I.Ls. are much rougher than the surface of SPES sample without I.Ls., as indicated by the RMS roughness values measured (Table 6). When I.Ls. are present, it is possible to observe that the surface at the air-side of the membrane remains smooth (*5e*). Conversely, the surface at the PTFE-side changes from smooth to rough (*5d*); RMS roughness data range from 66.65 nm for the air-side of the membrane to 185.15 nm for its PTFE- mold side.

The roughness of the PTFE-side of SPES_I.Ls. membranes increases as the DS of SPESs increases, i.e. with the number of the hydrophobic I.Ls. cations exchanged, as it is possible to observe comparing SPES_MEIM_0.5 (*5b*) with SPES_MEIM_0.75 (*5c*) and SPES_MEIM_1 (*5d*). This behavior was confirmed by RMS roughness values that for SPES_MEIM_0.5, SPES_MEIM_0.75 and SPES_MEIM_1 are 101.01 nm, 163.87 nm and 185.15 nm, respectively.

The influence of I.Ls. characterized by difference length of the imidazolinium alkyl chains was also investigated and the results obtained suggest that the roughness of the mold-side of SPES_I.Ls. membranes increases as the length of the imidazolinium alkyl chains increases, as shown in Figure 5e for SPES_MEIM_1 -RMS of 185.15 nm-, in Figure 5f for SPES_BBIM_1 -RMS of 192.78 nm-, in Figure 5g for SPES_MOIM_1 -RMS of 206.34 nm- and in Figure 5h for SPES_BOIM_1 -RMS of 236.85 nm-. As reported in the introduction, the control of surface morphology can enhance the

hydrophobicity of the material and, consequently, promote its self-cleaning performances.

In order to explain the differences observed between the air-side and the PTFE-mold side of SPES_I.Ls. films, Fourier Transform-Infrared (FT-IR) spectra were collected on both sides of the films in order to investigate a possible conformational rearrangement of I.Ls. on the surfaces of the polymeric membranes prepared.

Figure 6 shows FT-IR spectra of representative membranes from both air-side and PTFE-side of SPES_I.Ls. samples.

Comparing FT-IR spectra of SPES_MEIM membranes between the mold-side (Figure 6a) and the air-one (Figure 6b), it is possible to observe the presence of MEIM alkyl substituents peaks only on the mold-side surfaces: in fact, the absorption peaks between ~2800 cm^{-1} and 2950 cm^{-1} (1) are characteristic of the alkyl groups C-H stretching. The intensity of these absorption peaks gets higher as the length of I.Ls.alkyl chains increases (Figure 6c, d and e). FT-IR spectra of SPES_BBIM, SPES_MOIM and SPES_BOIM air-side samples show the same behavior of SPES_MEIM samples: they are reported in Supporting Information.

This behaviour indicates that a concentrated solution of SPES_I.L. behaves as a colloidal dispersion of molecules having apolar tails, i.e. imidazolinium alkyl chains, and polar heads, i.e. polymeric chains; in contact with a hydrophobic surface -the PTFE mold- the

apolar tails, less affine to the solvent, are orientated to the hydrophobic surface. Thanks to the selective orientation of the imidazolinium alkyl chains on the PTFE-side surface of all SPES_I.L. membranes the mold side is characterized by higher SWCAs and RMS data than the ones measured at the air-side of the membranes themselves.

4. CONCLUSIONS

The use of Sulfonated Polyarylethersulfones (SPESs), bearing sulfonic acid groups covalently bonded along the polymeric chain, is very advantageous in fields when the modulation of wetting properties is requested. Within this context, the use of Ionic Liquids (I.Ls.) combined with SPESs can be a way to create tailor-made hydrophobic materials.

In this work, a series of SPESs with different degree of sulfonation (DS) were successfully prepared via homogeneous synthesis. An ionic exchange reaction between the K^+ cation of the sulfonic comonomer of SPESs and different cationic apolar groups based I.Ls. was performed in order to modulate the wetting properties of SPESs; four different I.Ls. were synthesized with apolar alkyl chains characterized by increasing length: 1-Ethyl,3-Methyl Imidazolinium methyl sulfite (MEIM), 1,3-Dibutyl Imidazolinium bromide (BBIM), 1-Methyl,3-Octyl Imidazolinium bromide (MOIM) and 1-Butyl,3-Octyl Imidazolinium bromide (BOIM). SPES_I.Ls. samples were cast onto a PTFE mold to obtain membranes; wetting properties were measured both on the air-side surface and on the PTFE-side surface of the membranes themselves. Thanks to the addition of I.Ls., the hydrophobic properties measured on the PTFE-side surface increase

as the quantity of sulfonated groups increases, due to the higher number of I.Ls. cations exchanged. Increasing the length of the apolar alkyl chains of the I.Ls. cations, the static water contact angles increase: θ_w of SPES_MEIM_0.5 is $\overline{108}°$, a value that increases up to $\overline{123}°$ for SPES_BBIM_0.5, to $\overline{124}°$ for SPES_MOIM_0.5 and up to $\overline{130}°$ for SPES_BOIM_0.5. Furthermore, SWCA measurements on the air-side do not reveal significant differences changing DS and the length of the alkyl chains.

Combining SWCA data with both SEM and AFM analyses, it was possible to conclude that the increase of hydrophobic features on the mold-side for SPES_I.Ls. membranes with respect to the air-side is probably due to the organization of the apolar imidazolinium alkyl chains occurring during the evaporation of the solvent and to the interaction with high hydrophobic PTFE mold surface.

To the authors' best knowledge the present observation, i.e. of an induced roughness of the surface of films promoted by an ionic exchange reaction between cationic moieties of SPESs polymers and hydrophobic cationic I.L.s groups, has never been reported in previous scientific literature.

The work is continuing with an emphasis placed on the study of the influence of different processing conditions, such as solvent evaporation rate and processing temperatures on the properties of SPES_I.L.s films. Also other materials for molds, having different polarity, will be considered as an alternative to PTFE. Cation exchange reactions between

SPESs and I.L.s modified with fluorine based substituents will also be described in subsequent publications.

ACKNOWLEDGMENTS

This work has been carried out thanks to the financial support of Fondazione Cariplo for the project "Non Fluorinated polymeric membranes and platinum-free catalytic systems for Fuel-Cells (PEMFCs) with low cost and high efficiency". The authors wish to express their gratitude to Professor Giuseppe Di Silvestro (CRC Materiali Polimerici (LaMPo), Dipartimento di Chimica, Università degli Studi di Milano) for stimulating discussion and scientific projects. V.S. wish to express her gratitude to both Dr. Stefano Malacrida and Dr. Mirko Zappa for their experimental contributes.

REFERENCES

1. Yuan, Z., Huang, J., Peng, C., Wang, M., Wang, X., Bin, J., and Fu, X. Appl. Physics A, 122(2), 1-9, 2016. doi: 10.1007/s00339-016-9664-z.

2. Vafaei, S., Tuck, C., Ashcroft, I., and Wildman, R. Chem. Eng. Res. Design, 109, 414-420, 2016. doi: 10.1016/j.cherd.2016.02.004.

3. T. Dey, N. Daragh, J. Sol-Gel Sci. Technol. 77(1), 1-27, 2016. doi: 10.1007/s10971-015-3879-x.

4. Iwasaki, Y., and Kazuhiko, I., Sci. Tech. Advanced Mater. 13(6), 2012. doi: 10.1088/1468-6996/13/6/064101.

5. Wang, Z., Elimelech, M., and Lin, S. Environ. Sci. Tech. 50(5), 2132-2150, 2016. doi: 10.1021/acs.est.5b04351.

6. Rtimi, S., Pulgarin, C., Sanjines, R. and Kiwi, J. Appl. Catal., B 180, 648-655, 2016. doi:10.1016/j.apcatb.2015.06.047.

7. Smitha, V. S., Jaimy, K. B., Shajesh, P., Jeena, J. K. and Warrier, K. G. J. Mat. Chem. 1, 12641, 2013. doi:10.1039/c3ta12314f.

8. Wojciechowski, L., Kubiak, K. J. and Mathia, T.G. Tribol. Int. 93, 593-601, 2016. doi:10.1016/j.triboint.2015.04.013.

9. Qi, R., Hu, Y., Wang, Y. and Lu, L. J. Cleaner Prod. 112, 3555-3561, 2016. doi:10.1016/j.jclepro.2015.10.115.

10. Callies, M., Quéré, D. Soft Matter. 1, 55, 2005. doi:10.1039/b501657f.

11.Quéré, D. Annu. Rev. Mater. Res. 38, 71-99, 2008. doi:10.1146/annurev.matsci.38.060407.132434.

12. Jordan, J. H. and Gibb, B. C. Chem. Soc. Rev. 44(2), 547-585, 2015. doi:10.1039/C4CS00191E.

13. Liu, X., Wang, L., Hao, J. and Chu, L. Plasma Sci. Technol. 17, 2015. doi:10.1088/1009-0630/17/12/06.

14. Kato, K. and Yagami, H. Plasma vapor deposition, 1984, U.S. Patent No 4,446,168.

15. He, T., Wang, Y., Zhang, Y., Xu, T. and Liu, T. Corros. Sci. 51(8), 1757-1761, 2009. doi:10.1016/j.corsci.2009.04.027.

16. Marmur, A. Langmuir 19(20), 8343-8348, 2003. doi:10.1021/la0344682.

17. Nakajima, A., Abe, K., Hashimoto, K. and Watanabe, T. Thin Solid Films 376(1), 140-143, 2000. doi:10.1016/S0040-6090(00)01417-6.

18. Feng, L., Li, S., Li, Y., Li, H., Zhang, L., Zhai, J., Song, Y., Liu, B., Jiang, L. and Zhu, D. Adv. Mat. 14(24), 1857-1860, 2002. doi:10.1002/adma.200290020.

19. Chen, C., Wang, J. and Chen, Z. Langmuir 20(23), 10186-10193, 2004. doi: 10.1021/la049327u.

20. Giordano, S., Longhi, M., Formaro, L., Farina, H and Di Silvestro, G. J. Electrochem. Sci. Eng. 3(3), 115-123, 2013. 10.5599/jese.2013.0035

21. Gohil, G. S., Nagarale, R. H., Binsu, V. V. and Shahi, V. K. J. Colloid Interface Sci. 298(2), 845-853, 2006. doi: 10.1016/j.jcis.2005.12.069.

22. Falciola, L., Checchia, S., Pifferi, V., Farina, H., Ortenzi, M. A. and Sabatini V. Electrochim. Acta, 2016, doi.org/10.1016/j.electacta.2016.02.110.

23. Bai, P., Cao, X., Zhang, Y., Yin, Z., Wei, Q. and Zhao, C. J. Biomat. Sci. 21(12), 1559-1572, 2010. doi: 10.1163/092050609X12519805626158.

24. Balster, J., Krupenko, O., Pünt, I., Stamatialis, D. F and Wessling, M. J. Membr. Sci. 263(1), 137-145, 2005. doi: 10.1016/j.memsci.2005.04.019.

25. Kang, M. S., Choi, Y. J., Yoon, T. H. and Moon, S. H. J. Membr. Sci. 216(1), 39-53, 2003. doi: 10.1016/S0376-7388(03)00045-0.

26. Bikson, B., Coplan, M. J. and Gotz, G. Compositions and method of preparation by chlorosulfonation of difficultly sulfonatable poly (ether sulfone)U.S. Patent No 4, 508, 852, 1985.

27. Blanco, J. F, Nguyen, Q. T. and Schaetzel, P. J. Appl. Polym. Sci. 84(13), 2461-2473, 2002. doi: 10.1002/app.10536.

28. Jutemar, E. P. and Jannasch, P. J. Membr. Sci. 351(1-2), 87–95, 2010. doi:10.1016/j.memsci.2010.01. 036.

29. Harrison, W. L., Wang, F., Mecham, J. B., Bhanu, V. A., Hill, M., Kim, Y. S. and McGrath, J. E. J. Polym. Sci., Part A: Polym. Chem. 41 (14), 2264–2276, 2003. doi:10.1002/pola.10755.

30. Higashihara, T., Matsumoto, K. and Ueda, M. Polym. 50(23), 5341–5357, 2009. doi:10.1016/j.polymer.2009.09.001.

31. Sabatini, V., Checchia, S., Farina, H., Ortenzi, M. A. Macromolecular. Research. 2016, Accepted, in press.

32. Welton, T. Chem. Rev. 99(8), 2071-2084, 1999. doi:10.1021/cr980032t.

33. Fuller, J., Breda, A. C. and Carlin, R. T. J. Electrochem. Soc. 144(4), L67-L70, 1997. doi:10.1149/1.1837555.

34. Huddleston, J. G., Visser, A. E., Reichert, W. M., Willaeur, H. D., Broker, G. A. and Rogers, R. D. Green Chem. 3(4), 156-164, 2001. doi:10.1039/B103275P.

35. Tokuda, H., Hayamizu, K., Ishii, K., Susan, M. A. B. H. and Watanabe, M. J. Physic. Chem., B 109(13), 6103-6110, 2005. doi:10.1021/jp044626d.

36. Soliveri, G., Sabatini, V., Farina, H., Ortenzi, M. A., Meroni, D., Colombo, A. *Colloid. Surf. A: Physochem. Eng. Asp.* 483, 28-291, 2015. doi:10.1016/j.colsurfa.2015.06.059.

37. Wilkes, J. S., Levisky, J. A., Wilson, R. A. and Hussey, C. L. Inorg. Chem. 21(3), 1263-1264, 1982. doi: 10.1021/ic00133a078.

38. Browne, C., Tabor, R. F., Grieser, F., Dagastine, R. R. J. Colloid. Inter. Sci. 1, 449, 236-245, 2015. doi: 10.1016/j.jcis.2014.12.076.

39. Li, Y., Wang, F., Yang, J., Liu, D., Roy, A., Case, S., Lesko, J., McGrath, J. Polymer, 47, 11, 2006. doi: 10.1016/j.polymer.2006.03.003.

40. Wang, L. R., Qin, H., Nie, S. Q., Sun, S. D., Ran, F., Zhao, C. S. Acta Biomat. 9, 8851-8863, 2013. doi: 10.1016/j.actbio.2013.07.010.

41. Harrison, W. L., Hickner, M. A., Kim, Y. S and McGrath, J. E. Fuel Cells 5(2), 201-212, 2005. doi: 10.1002/fuce.200400084.

42. Wang, M., Wu, L. G., Mo, J. X and Gao, C. J. J. Membr. Sci. 274(1), 200-208, 2006. doi: 10.1016/j.memsci.2005.05.035.

43. Yeo, J. K., Sperling, L. H. and Thomas, D. A. Polym. Eng. Sci. 21(11), 696-702, 1981. doi: 10.1002/pen.760211111.

Table 1. Loading of the reagents for SPESs with different DS.

Samples	nominal DS (meq SO_3*g^{-1} of polymer)	BFPS (g)	BHP (g)	SHQ (g)	K_2CO_3 (g)
SPES_0.5	0.5	3.17	1.85	0.58	3.72
SPES_0.75	0.75	3.15	1.69	0.76	3.70
SPES_1	1	3.10	1.32	1.16	3.64

Table 2. Amounts of the reagents adopted for the syntheses of SPES_I.Ls.

Samples	^{1}H NMR DS (meq SO_3*g^{-1} of polymer)	SPES (g)	I.L. (g)
SPES_MEIM_0.5	0.48	0.90	0.20
SPES_MEIM_0.75	0.70	0.90	0.29
SPES_MEIM_1	0.98	0.90	0.41
SPES_BBIM_0.5	0.48	0.90	0.25
SPES_BBIM_0.75	0.70	0.90	0.37
SPES_BBIM_1	0.98	0.90	0.52
SPES_MOIM_0.5	0.48	0.90	0.27
SPES_MOIM_0.75	0.70	0.90	0.39
SPES_MOIM_1	0.98	0.90	0.55
SPES_BOIM_0.5	0.48	0.90	0.36
SPES_BOIM_0.75	0.70	0.90	0.53
SPES_BOIM_1	0.98	0.90	0.74

Table 3. List of SPESs synthesized with their DS, intrinsic values (η), SEC data and T_g values.

Samples	nominal DS (meq SO_3^-*g^{-1} of polymer)	^{1}H NMR DS (meq SO_3^-*g^{-1} of polymer)	[η] ($dL*g^{-1}$)	$\overline{Mn}$ (Da)	$\overline{Mw}$ (Da)	D	T_g (°C)
SPES_0.5	0.5	0.48	0.34	23727	43460	1.83	259.7
SPES_0.75	0.75	0.70	0.49	25431	48573	1.91	290.9
SPES_1	1	0.98	0.72	26679	52870	1.98	303.6

Table 4. List of SPES_I.Ls. synthesized with their RS and T_g data.

Samples	^{1}H NMR RS (%)	T_g (°C)
SPES_MEIM_0.5	81	247.9
SPES_MEIM_0.75	68	286.1
SPES_MEIM_1	78	299.5
SPES_BBIM_0.5	96	252.3
SPES_BBIM_0.75	87	263.2
SPES_BBIM_1	94	272.4
SPES_MOIM_0.5	97	249.5
SPES_MOIM_0.75	98	299.4
SPES_MOIM_1	98	292.3
SPES_BOIM_0.5	98	246.1
SPES_BOIM_0.75	90	298.4
SPES_BOIM_1	97	280.6

Table 5. SWCA of SPESs and SPES_I.Ls.

Samples	θ_w (air-side)	θ_w (PTFE-side)
SPES_0.5	$\overline{69}\pm1$	$\overline{83}\pm2$
SPES_0.75	$\overline{60}\pm1$	$\overline{74}\pm1$
SPES_1	$\overline{53}\pm1$	$\overline{59}\pm1$
SPES_MEIM_0.5	$\overline{86}\pm2$	$\overline{108}\pm1$
SPES_MEIM_0.75	$\overline{85}\pm1$	$\overline{116}\pm1$
SPES_MEIM_1	$\overline{89}\pm1$	$\overline{121}\pm1$
SPES_BBIM_0.5	$\overline{88}\pm1$	$\overline{123}\pm1$
SPES_BBIM_0.75	$\overline{84}\pm2$	$\overline{124}\pm2$
SPES_BBIM_1	$\overline{81}\pm2$	$\overline{126}\pm1$
SPES_MOIM_0.5	$\overline{77}\pm1$	$\overline{124}\pm1$
SPES_MOIM_0.75	$\overline{80}\pm1$	$\overline{125}\pm2$
SPES_MOIM_1	$\overline{81}\pm1$	$\overline{128}\pm1$
SPES_BOIM_0.5	$\overline{85}\pm1$	$\overline{130}\pm1$
SPES_BOIM_0.75	$\overline{80}\pm1$	$\overline{131}\pm1$
SPES_BOIM_1	$\overline{81}\pm1$	$\overline{131}\pm1$

Table 6. RMS roughness values of SPESs and SPES.I.Ls. samples.

Samples	air-side RMS (nm)	PTFE-side RMS (nm)
SPES_1	45.55	67.27
SPES_MEIM_0.5	46.41	101.01
SPES_MEIM_0.75	60.38	163.87
SPES_MEIM_1	66.65	185.15
SPES_BBIM_1	87.89	192.78
SPES_MOIM_1	88.53	206.34
SPES_BOIM_1	93.22	236.85

Scheme 1.

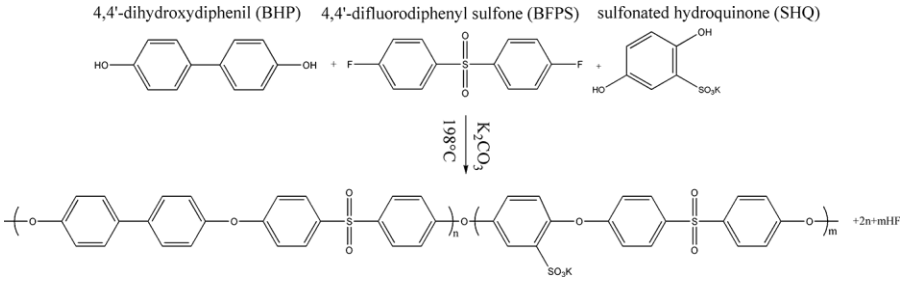

Scheme 2.

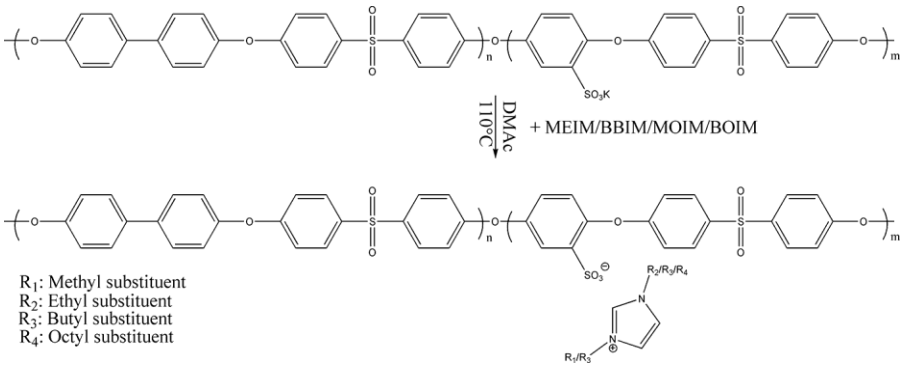

R_1: Methyl substituent
R_2: Ethyl substituent
R_3: Butyl substituent
R_4: Octyl substituent

Figure 1.

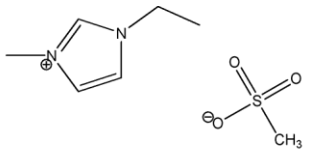

1-Ethyl, 3-Methyl Imidazolinium methyl sulfite (MEIM)

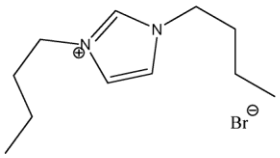

1,3-Dibutyl Imidazolinium bromide (BBIM)

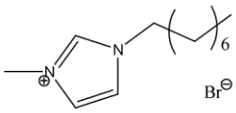

1-Methyl, 3-Octyl Imidazolinium bromide (MOIM)

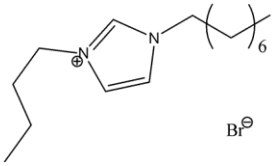

1-Butyl, 3-Octyl Imidazolinium bromide (BOIM)

Figure 2.

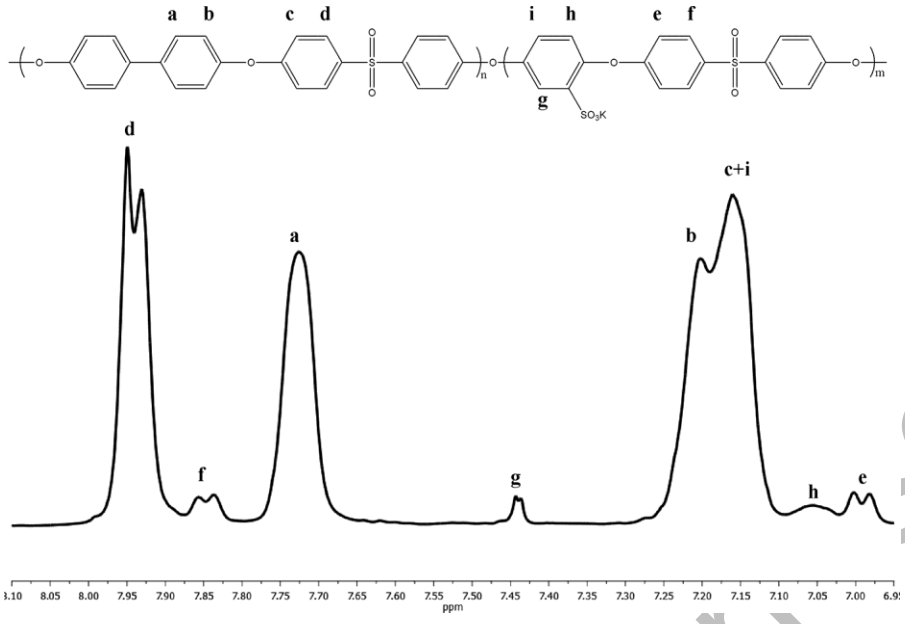

Figure 3.

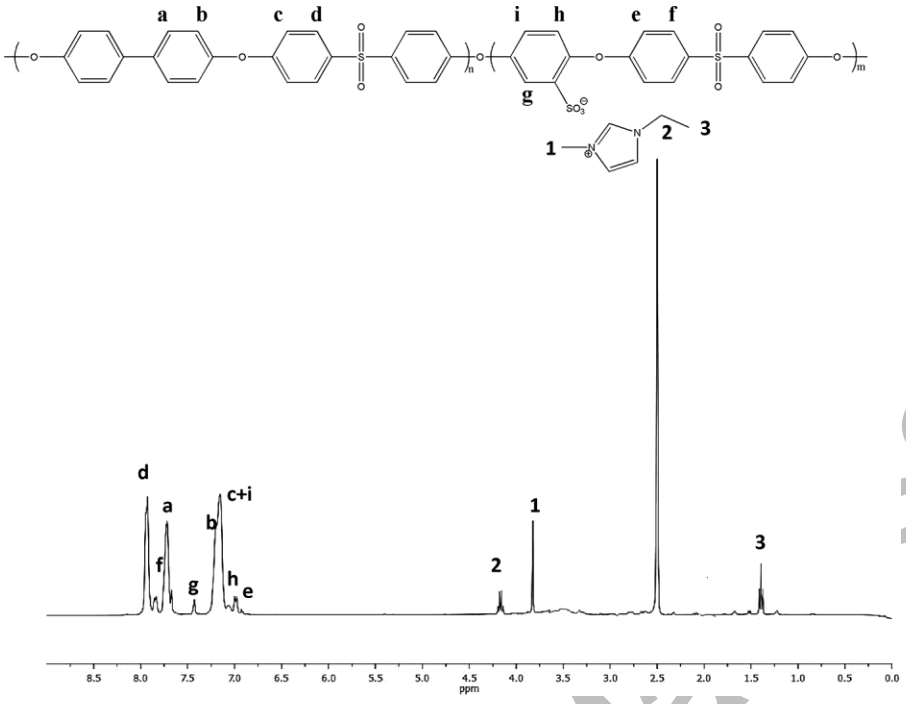

Figure 4.

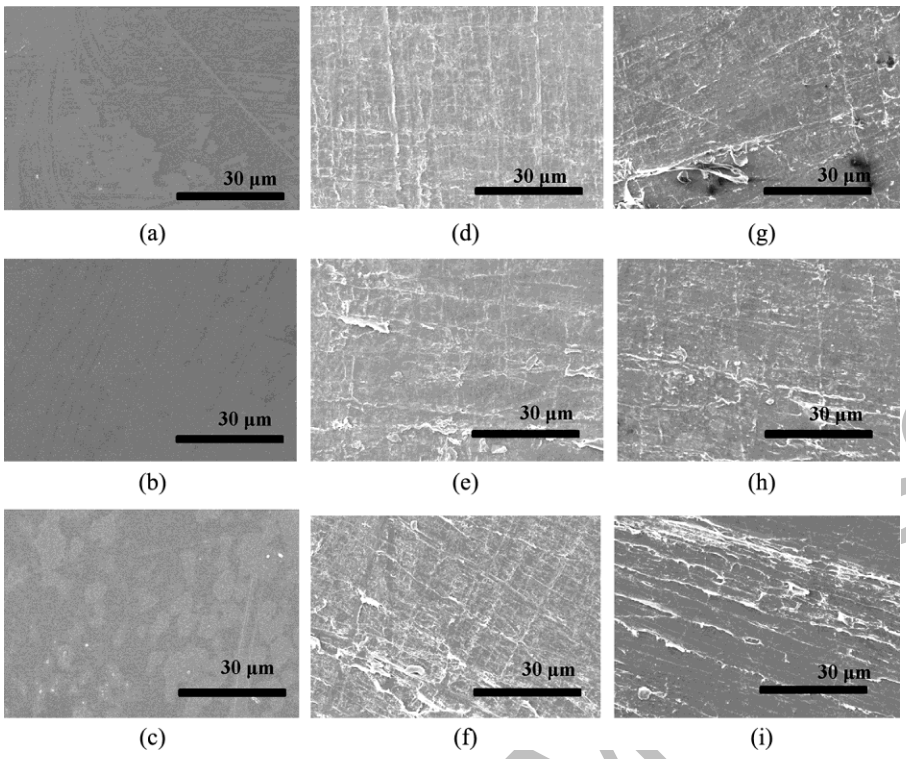

Figure 5.

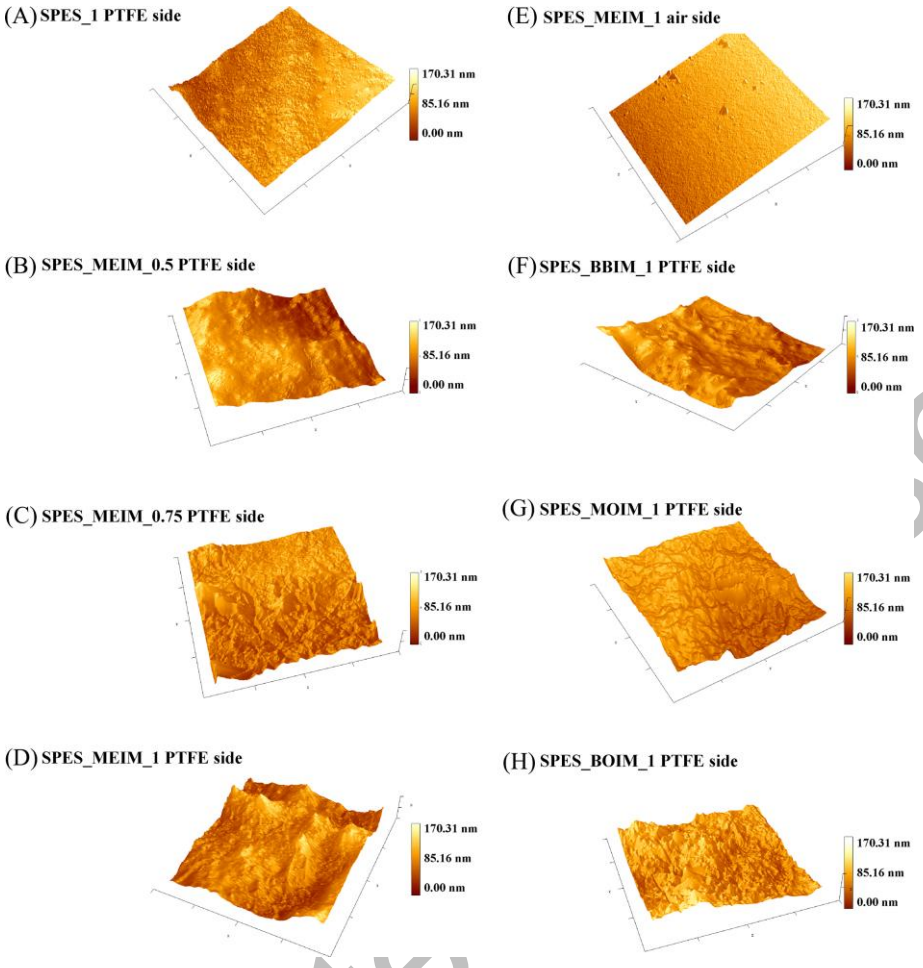

Figure 6.